Interpretation of visible moiré between repetitive periodic-like gratings in the image domain

Lei Yu,* Shu-Rong Wang, and Guan-Yu Lin

Changchun Institute of Optics, Fine Mechanics and Physics, Chinese Academy of Sciences, Changchun 130033, China

*Corresponding author: top1gods@mail.ustc.edu.cn

Received 11 June 2014; revised 10 August 2014; accepted 11 August 2014;
posted 12 August 2014 (Doc. ID 213704); published 2 December 2014

An image domain approach to the interpretation of visible moiré phenomena in repetitive grating multiplicative superposition has been proposed. The local frequency method provides the instantaneous period and orientation of generated moiré. These parameters of the moiré have been sorted into real and pseudo patterns by the Fourier expansions analysis. With the combination of these two steps, the concept "equivalent period contribution threshold" has been introduced. It is found that different thresholds bring different integral domains and results for the calculation of average intensities of generated moiré waveforms. This proves that different thresholds would introduce different average intensity distribution (macrostructure effects) in different moiré patterns. With the local intensity variation (microstructure effects), the human eye would confuse different macrostructure effects but only consider them the same. The interpretation is that the macrostructure versus microstructure effects garble discernment of the human eye and result in different visible moiré phenomena. This is significant for visible moiré effects in various repetitive grating (both of cosinusoidal and binary patterns) superpositions in the image domain. It also presents and summarizes the coexistence of real and pseudo moirés in repetitive, periodic-like layer superposition.

OCIS codes: (120.4120) Moiré techniques; (070.0070) Fourier optics and signal processing; (050.2770) Gratings.

http://dx.doi.org/10.1364/AO.53.008197

1. Introduction

The moiré phenomenon was first discovered in France. The first scientific research was made by Lord Rayleigh [1]. Generally, the superposition of two or more periodic (or quasi-periodic) structures leads to a coarser structure, which is the appearance of interfering patterns named moiré pattern or moiré fringe [2,3]. There are two aspects, moiré pattern analysis and moiré pattern synthesis, in modern moiré research [4–6].

A phenomenon called pseudo moiré is one that the human eye can receive, but Fourier theory hardly captures. Amidror presented a combination of points in the theoretical prediction of visible moiré effects [7]. Kong *et al.* [8] interpreted the phenomenon with the consideration of illusional contrast of human visual systems. Patorski *et al.* [9] used the concept of biased and unbiased frequency pairs to interpret the real and pseudo moiré in the Fourier domain based on the notion of detectable intensity modulations. Yu *et al.* [10] presented a visible moiré explanation both for cosinusoidal and binary gratings in the multiplicative and additive superpositions. These studies mainly focus on the superposition of periodic straight gratings but not the repetitive, periodic-like layers.

Visible moiré is not limited to the superposition of periodic layers, and indeed often occurs between other types of repetitive structures (namely, geometrically transformed periodic layers). Amidror [11] has studied the moiré patterns qualitatively as well as quantitatively with various mathematical tools,

1559-128X/14/358197-08$15.00/0

both in the image and the Fourier spectral domain. In the application, three main types of periodic-like, repetitive layer structures are usually used as coordinate-transformed structures, profile-transformed structures, and coordinate- and profile-transformed structures. As their names indicate, such structures can be obtained from a certain initial periodic structure by the application of a coordinate transformation (as in the case of a curvilinear grating), a profile transformation (as in the case of a screen gradation), or a combination of both.

In Section 2, the local frequency method is introduced first to obtain the instantaneous periods and orientations of the generated moiré. This solves the problem that the moiré in repetitive layer superposition is hard to present in mathematical forms. Then Fourier analysis is utilized to express the new generated terms for moiré; it presents the abecedarian distinction of real and pseudo moiré. With these two methods, the real and pseudo moiré are made distinct by different parameters, and the concept of "equivalent period contribution threshold" has been provided in the calculation in Section 2.C. The concept of thresholds is a novelty and helps us to calculate the average intensity of the generated moiré. The problem introduced by the variation of periods of moiré, that the average moiré intensity is difficult to calculate, has been solved by the threshold concept. By this calculation and the analysis in this work, the interpretation of visible moiré in periodic-like, repetitive grating superposition in the image domain is obtained such that the interaction of average intensity variation (macrostructure effects) and local intensity variation (microstructure effects) under different "thresholds" produces the generation of visible real and pseudo moiré. Sections 3 and 4 present the example of cosinusoidal grating and binary grating superposition to prove our interpretation. These two sections also prove the coexistence of two moiré patterns. In general, the mathematical method in our research has never been used in the generated moiré in repetitive, periodic-like grating superposition, and it proves that the method would be suitable for interpreting real and pseudo moiré patterns.

2. Interpretation of the Multiplicative Superposition of Cosinusoidal Repetitive, Periodic-like Gratings

As referred to in the preceding section, the coordinate-transformed structures present special interest in the engineering application. Therefore, we will mainly discuss the superposition of co-ordinate-transformed structures in the following sections. To simplify the research, the repetitive, periodic-like grating can be expressed in the simple case of coordinate-transformed structures, that of curvilinear gratings. Let $r(x,y)$ be the curvilinear grating which is obtained by bending the 2D one-fold periodic grating $p(x')$ by replacing x' with the function $g(x,y)$:$r(x,y) = p(g(x,y))$. Without loss of generality, the grating $p(x')$ is made as the 2D cosinusoidal grating for the sake of convenience in the application. Namely, the grating can be expressed as $r(x,y) = p(g(x,y)) = \cos(2\pi f g(x,y))$.

A. Calculation of Parameters of the Moiré in the Image Domain

Our analysis is based on the local frequency method, which only involves the image domain. The indicial equations method [12] hardly obtains the period and orientation of moiré in the repetitive, periodic-like grating superposition for the variation of them. Therefore, the local frequency method will be utilized. It is based on considering each of the superposed structures as locally straight and locally periodic in every infinitesimally small region, and studying the locally straight, periodic moirés that are generated in each such region. In other words, each curvilinear grating is approximated in any infinitesimally small region by the straight, periodic grating which is tangential to it and which has the same periodic profile. The local frequency vector at any point (x, y) of $r(x,y)$ is given by the gradient as the method shows:

$$\vec{f}(x,y) = \left(f\frac{\partial}{\partial x}g(x,y), f\frac{\partial}{\partial y}g(x,y)\right). \tag{1}$$

The local frequency vectors of the two superposed gratings r_1 and r_2 will be given by

$$\begin{cases} \vec{f}_1 = \left(f_1\frac{\partial}{\partial x}g_1(x,y), f_1\frac{\partial}{\partial y}g_1(x,y)\right) \\ \vec{f}_2 = \left(f_2\frac{\partial}{\partial x}g_2(x,y), f_2\frac{\partial}{\partial y}g_2(x,y)\right) \end{cases}. \tag{2}$$

The local frequency vector of the generated $(k_1, \pm k_2)$ moiré in the multiplicative superposition of $r_1 \times r_2$ is

$$\vec{f}_{k_1,\pm k_2} = \left(k_1 f_1\frac{\partial}{\partial x}g_1(x,y) \pm k_2 f_2\frac{\partial}{\partial x}g_2(x,y), k_1 f_1\frac{\partial}{\partial y}g_1(x,y) \pm k_2 f_2\frac{\partial}{\partial y}g_2(x,y)\right). \tag{3}$$

The local frequency vector can be exchanged into the local period vector expression as

$$\vec{T}_{k_1,\pm k_2} = \left(\frac{T_1T_2}{k_1T_2\frac{\partial}{\partial x}g_1(x,y) \pm k_2T_1\frac{\partial}{\partial x}g_2(x,y)}, \frac{T_1T_2}{k_1T_2\frac{\partial}{\partial y}g_1(x,y) \pm k_2T_1\frac{\partial}{\partial y}g_2(x,y)}\right)\left(T_1 = \frac{1}{f_1}, T_2 = \frac{1}{f_2}\right). \tag{4}$$

The local parameters will also be called instantaneous parameters. The modulus of the instantaneous period of moiré is

$$|T_{k_1,\pm k_2}| = \frac{T_1 T_2}{\sqrt{\left(k_1 T_2 \frac{\partial}{\partial x} g_1(x,y) \pm k_2 T_1 \frac{\partial}{\partial x} g_2(x,y)\right)^2 + \left(k_1 T_2 \frac{\partial}{\partial y} g_1(x,y) \pm k_2 T_1 \frac{\partial}{\partial y} g_2(x,y)\right)^2}}. \tag{5}$$

We can also obtain the expression of the instantaneous orientation of the moiré,

$$\cos\gamma = \frac{k_1 T_2 \frac{\partial}{\partial y} g_1(x,y) \pm k_2 T_1 \frac{\partial}{\partial y} g_2(x,y)}{\sqrt{\left(k_1 T_2 \frac{\partial}{\partial x} g_1(x,y) \pm k_2 T_1 \frac{\partial}{\partial x} g_2(x,y)\right)^2 + \left(k_1 T_2 \frac{\partial}{\partial y} g_1(x,y) \pm k_2 T_1 \frac{\partial}{\partial y} g_2(x,y)\right)^2}}. \tag{6}$$

B. Discrimination of Generated Moiré by the Fourier Series Expansion

For the symmetry of $r(x,y) = p(x') = \cos(2\pi f g(x,y))$, the Fourier series expansion of it becomes

$$p(x') = \frac{a_0}{2} + \sum_{n=1}^{\infty} a_n \cos\frac{2n\pi x'}{T}. \tag{7}$$

The coefficients are

$$\begin{cases} a_0 = 1 \\ a_n = \frac{4}{T}\int_0^{\frac{T}{2}} p(x')\cos\frac{2n\pi x'}{T}\,dx' = \frac{4}{T}\int_0^{\frac{T}{2}} \cos\left(\frac{2\pi}{T}x'\right)\cos\frac{2n\pi x'}{T}\,dx' (n = 1,2,3,\ldots) \end{cases}. \tag{8}$$

We replace x' in the Fourier series with the function $g(x,y)$, which defines the curvilinear behavior of the grating $r(x,y)$ throughout the plane. Expressions of two superposed cosinusoidal curvilinear gratings are

$$\begin{cases} r_1(x,y) = \frac{a_0^1}{2} + \sum_{m=1}^{\infty} a_m^1 \cos\frac{2m\pi g_1(x,y)}{T_1} \\ r_2(x,y) = \frac{a_0^2}{2} + \sum_{n=1}^{\infty} a_n^2 \cos\frac{2n\pi g_2(x,y)}{T_2} \end{cases}, \tag{9}$$

with the same coefficients a_n as Expression (8).

The multiplicative superposition $r_1(x,y) \times r_2(x,y)$ can be expressed as

$$\begin{aligned} r_1 \times r_2 = \frac{1}{2}\Bigg[& \frac{a_0^1 a_0^2}{2} + a_0^1 \sum_{n=1}^{\infty} a_n^2 \cos\frac{2n\pi g_2(x,y)}{T_2} \\ & + a_0^2 \sum_{m=1}^{\infty} a_m^1 \cos\frac{2m\pi_1 g_1(x,y)}{T_1} + \sum_{m=1}^{\infty}\sum_{n=1}^{\infty} a_m^1 a_n^2 \\ & \times \cos 2\pi\left(\frac{m g_1(x,y)}{T_1} + \frac{n g_2(x,y)}{T_2}\right) \\ & + \sum_{m=1}^{\infty}\sum_{n=1}^{\infty} a_m^1 a_n^2 \cos 2\pi\left(\frac{m g_1(x,y)}{T_1} - \frac{n g_2(x,y)}{T_2}\right)\Bigg]. \end{aligned} \tag{10}$$

The partial sum which corresponds to the $(k_1, \pm k_2)$ moiré consists of all the terms of this multiple sum whose indices are $n'k_1$, $\pm n'k_2$, namely

$$\begin{aligned} m_{k_1,\pm k_2} &= \frac{1}{2}\sum_{m=1}^{\infty}\sum_{n=1}^{\infty} a_m^1 a_n^2 \cos 2\pi\left(\frac{m g_1(x,y)}{T_1} \pm \frac{n g_2(x,y)}{T_2}\right) \\ &= \frac{1}{2}\sum_{n'=1}^{\infty} a_{n'k_1}^1 a_{n'k_2}^2 \cos 2\pi n'\left(\frac{k_1 g_1(x,y)}{T_1} \pm \frac{k_2 g_2(x,y)}{T_2}\right), \end{aligned} \tag{11}$$

According to Expression (8), the coefficients in r_1 and r_2 are

$$\begin{aligned} & a_0^1 = a_0^2 = 1, \qquad a_{n'k_1}^1 = \begin{cases} \frac{1}{2}(k_1 = 1) \\ 0(k_1 > 1) \end{cases}, \\ & a_{n'k_2}^2 = \begin{cases} \frac{1}{2}(k_2 = 1) \\ 0(k_2 > 1) \end{cases}. \end{aligned} \tag{12}$$

It is evident that the terms of Expression (11) will be zero when the coefficients $a_{n'k_1}^1$ or $a_{n'k_2}^2$ are zero on the condition of $k_1 > 1$ or $k_2 > 1$. Therefore, the simplified expression of $(k_1, \pm k_2)$ moiré term $m_{k_1 k_2}$ becomes

$$m_{1,\pm 1} = \frac{1}{8}\cos[2\pi(f_1 g_1(x,y) \pm f_2 g_2(x,y))]. \tag{13}$$

By the just-shown Fourier series expansion of the generated moiré in the multiplicative superposition, it could be acceptable that only the term $m_{1,\pm 1}$ is kept, but the other terms of this multiple partial sum term whose indices are larger than one are zero. Therefore, it is considered that there only exists the $(1, \pm 1)$ moiré in the Fourier analysis. When $k_1 > 1$ or $k_2 > 1$, the coefficients of new generated terms in the Fourier expansion are zero. This means that the

amplitudes of the generated impulses of these terms of the moiré in the frequency domain of the superposition are zero. At this time, the Fourier analysis would not capture these "zero" impulses, but the effect of these terms may be received by the human visual system. Furthermore, when this phenomenon, which doesn't belong to the effects introduced by the terms $m_{1,\pm1}$ (the coefficients $k_1 > 1$ or $k_2 > 1$), is received by human eye, the pseudo moiré would be generated.

C. Parameter Analysis of Real and Pseudo Moiré

1. *Real Moiré [(1, ±1) Moiré]*

According to the calculation in Sections 2.A and 2.B, the (1, ±1) moiré is the real moiré. At the moment, the parameters of real moiré are

$$\begin{cases} |T_r| = T_1T_2\left(\frac{1}{\left(T_2\frac{\partial}{\partial x}g_1(x,y)\pm T_1\frac{\partial}{\partial x}g_2(x,y)\right)^2}+\frac{1}{\left(T_2\frac{\partial}{\partial y}g_1(x,y)\pm T_1\frac{\partial}{\partial y}g_2(x,y)\right)^2}\right)^{\frac{1}{2}} \\ \cos\gamma_r = \frac{T_2\frac{\partial}{\partial y}g_1(x,y)\pm T_1\frac{\partial}{\partial y}g_2(x,y)}{\sqrt{\left(T_2\frac{\partial}{\partial x}g_1(x,y)\pm T_1\frac{\partial}{\partial x}g_2(x,y)\right)^2+\left(T_2\frac{\partial}{\partial y}g_1(x,y)\pm T_1\frac{\partial}{\partial y}g_2(x,y)\right)^2}} \end{cases}. \tag{14}$$

2. *Pseudo Moiré [(k_1, ±k_2) Moiré, $k_1 \neq k_2$]*

In this situation, the parameters of pseudo moiré are

$$\begin{cases} |T_p| = T_1T_2\left(\frac{1}{\left(k_1T_2\frac{\partial}{\partial x}g_1(x,y)\pm k_2T_1\frac{\partial}{\partial x}g_2(x,y)\right)^2}+\frac{1}{\left(k_1T_2\frac{\partial}{\partial y}g_1(x,y)\pm k_2T_1\frac{\partial}{\partial y}g_2(x,y)\right)^2}\right)^{\frac{1}{2}} \\ \cos\gamma_p = \frac{k_1T_2\frac{\partial}{\partial y}g_1(x,y)\pm k_2T_1\frac{\partial}{\partial y}g_2(x,y)}{\sqrt{\left(k_1T_2\frac{\partial}{\partial x}g_1(x,y)\pm k_2T_1\frac{\partial}{\partial x}g_2(x,y)\right)^2+\left(k_1T_2\frac{\partial}{\partial y}g_1(x,y)\pm k_2T_1\frac{\partial}{\partial y}g_2(x,y)\right)^2}} \end{cases}. \tag{15}$$

$|T'_1|$ and $|T'_2|$ are the corresponding equivalent periods of r_1 and r_2, which are projection periods on the orientation of the generated moiré. These periods will be considered as equivalent periods of two gratings in the generated moiré. Then we have

$$\frac{|T'_1|}{|T'_2|} = \frac{k_1}{k_2}. \tag{16}$$

According to the preceding discussion, when the ratio is equal to one, the generated moiré is real moiré; when it is not equal to one, it is pseudo moiré. Therefore, we call the ratio the "equivalent period contribution threshold," which defines contributions of equivalent periods for the generated moiré.

D. Heuristic Interpretation of the Physical Meaning

For the sake of convenience, we will make simplifications for the grating waveform average intensity calculation. First, in the generated waveform r as the product of the two gratings r_1 and r_2, the variation of instantaneous moiré orientation does not influence the intensity (e.g., the value of amplitude in the 2D spectrum). Therefore, the 2D waveform r of the generated moiré could be unfolded into the 1D waveform r' in a line for the average intensity calculation without any error. At this time, the orientation of the period of waveform is along the new X axis, and the waveform becomes a 1D waveform. Second, by the first establishment, the term $g(x,y)$ will be replaced with x' and $p(g(x,y)) = \cos(2\pi f g(x,y))$ will become $p(x') = \cos(2\pi f x')$. Under the transformation, the function $g(x,y)$ is replaced by x' in the X direction. This will make the calculation for average intensity more convenient. Gratings r_1 and r_2 are expressed as

$$\begin{cases} r_1 = \frac{1}{2}\cos\left(\frac{2\pi}{T_1}g_1(x,y)\right)+\frac{1}{2} \\ r_2 = \frac{1}{2}\cos\left(\frac{2\pi}{T_2}g_2(x,y)\right)+\frac{1}{2} \end{cases}. \tag{17}$$

The two projections of waveforms will be first expressed in the 1D case along the unfolded new X axis direction as

$$\begin{cases} r'_1 = \frac{1}{2}\cos\frac{2\pi}{|T'_1|}(x'+\theta_1)+\frac{1}{2} \\ r'_2 = \frac{1}{2}\cos\frac{2\pi}{|T'_2|}(x'+\theta_2)+\frac{1}{2} \end{cases}, \tag{18}$$

where $|T'_1|$ and $|T'_2|$ are the equivalent periods (projected periods on the generated moiré orientation) of r'_1 and r'_2 [as in Expression (16)]. θ_1 and θ_2 are arbitrary angular displacements of r'_1 and r'_2. The variations of them stand for different waveforms in the parallel waveform family of superposed gratings. The new waveform r' of the generated moiré could be expressed as

$$\begin{aligned} r' = r'_1 \times r'_2 &= \frac{1}{4}+\frac{1}{4}\cos\frac{2\pi}{|T'_1|}(x'+\theta_1) \\ &+\frac{1}{4}\cos\frac{2\pi}{|T'_2|}(x'+\theta_2)+\frac{1}{8}\Bigg[\cos 2\pi\left(\frac{|T'_1|+|T'_2|}{|T'_1||T'_2|}\right) \\ &\times\left(x'+\frac{1}{|T'_1|+|T'_2|}(|T'_2|\theta_1+|T'_1|\theta_2)\right) \\ &+\cos 2\pi\left(\frac{|T'_2|-|T'_1|}{|T'_1||T'_2|}\right) \\ &\times\left(x'+\frac{1}{|T'_2|-|T'_1|}(|T'_2|\theta_1-|T'_1|\theta_2)\right)\Bigg]. \end{aligned} \tag{19}$$

The fluctuations of average intensity of each waveform can be calculated by the conventional integral method.

1. Real Moiré

When the threshold is equal to one, the integral period is chosen as $|T'| = |T'_1| = |T'_2|$. Then Expression (19) can be changed to

$$r' = \frac{1}{4} + \frac{1}{4}\cos\left(\frac{2\pi}{|T'|}x' + \theta_1\right) + \frac{1}{4}\cos\left(\frac{2\pi}{|T'|}x' + \theta_2\right) + \frac{1}{8}\cos\frac{2\pi}{|T'|}(2x' + \theta_1 + \theta_2) + \frac{1}{8}\cos\frac{2\pi}{|T'|}(\theta_1 - \theta_2). \tag{20}$$

The average intensity of waveform is calculated as

$$I_{\text{aver}} = \frac{1}{|T'|}\int_0^{|T'|} r' \mathrm{d}x' = \frac{1}{8}\cos\frac{2\pi}{|T'|}(\theta_1 - \theta_2) + \frac{1}{4}. \tag{21}$$

It is obvious that the average intensity of waveform along the orientation of the real moiré is changing with the variation of θ_1 and θ_2.

2. Pseudo Moiré

When the threshold is not equal to one, the integral period is chosen as the least common multiple $|T'|$ of $|T'_1|$ and $|T'_2|$:

$$r' = \frac{1}{4} + \frac{1}{4}\cos\frac{2m\pi}{|T'|}(x' + \theta_1) + \frac{1}{4}\cos\frac{2n\pi}{|T'|}(x' + \theta_2) + \frac{1}{8}\left[\cos\frac{2\pi}{|T'|}((m+n)x' + m\theta_1 + n\theta_2) + \cos\frac{2\pi}{|T'|}((m-n)x' + m\theta_1 - n\theta_2)\right]. \tag{22}$$

Then the average intensity of waveform is calculated as

$$I_{\text{aver}} = \frac{1}{|T'|}\int_0^{|T'|} r' \mathrm{d}x' = \frac{1}{4}. \tag{23}$$

According to the just-discussed research, when the average intensity of different parallel waveforms along the orientation of moiré in the superposition r' changes with parameters θ_1 and θ_2, the generated moiré is real moiré. On the contrary, when the average intensity stays constant, the generated moiré is pseudo moiré. This leads to the conclusion that different thresholds determine different average intensities of waveforms which belong to different visible moiré in the multiplicative superposition. Effects generated by thresholds which introduce the visible real and pseudo moiré to the human visual system can be boiled down to the macrostructure versus microstructure effect.

When the threshold is equal to one, the equivalent periods $|T'_1|$ and $|T'_2|$ will contribute the same effects to the generated waveforms along the real moiré orientation. At this time, the average intensity of waveform will present a similar cosinusoidal profile as the cosinusoidal variation of local intensity. In other words, the variations of average intensity (macrostructure) and local intensity (microstructure) remain synchronous. When the human visual system captures the "real synchronous" phenomenon, the real moiré happens in the superposition. When the threshold is not equal to one, the equivalent periods $|T'_1|$ and $|T'_2|$ will contribute different effects to the generated waveforms along the pseudo moiré orientation. This effect keeps the average intensity of waveforms constant, but the variation of local intensity still presents the cosinusoidal characteristics; namely, macrostructure effects don't accord with microstructure effects. However, with cosinusoidal variation of local intensity, the human eye will hardly discern the constant average intensity (macrostructure effects) and consider that the average intensity variation keeps synchronous with the intensity variation. Under the "pseudo synchronism," the adjacent local intensity variations will be connected into the moiré-like band by the human eye, and the pseudo moiré generates.

Kong *et al.* [8] proposed the concept of illusional contrast in the cosinusoidal periodic straight grating superposition, which is one special situation in our study. In fact, no matter how the periods of superposed gratings vary, the influence of essential factor "equivalent period contribution threshold" would be impervious to the period variation, but only the ratio of periods. The macrostructure versus microstructure effects which are caused by the different threshold introduce the real and pseudo moiré to the human visual system. It also proves that the human eye is more sensitive to the microstructure effects than Fourier analysis.

An important conclusion could be obtained from this discussion that the real moiré and pseudo moiré may coexist and appear in the same superposition. This is because the periods of different grating layers will contribute effects both in real and pseudo moiré orientations simultaneously. However, the human eye usually accepts only one visible moiré effect even if the two visible moiré coexist. More detailed analysis of the coexistence of real and pseudo moiré will be discussed in Section 3 to interpret which moiré the human eye is more sensitive to under different thresholds.

3. Simulations and Discussion of the Coexistence of Real Moiré and Pseudo Moiré

The coexistence of real moiré and pseudo moiré in the multiplicative superposition will be discussed. Here, we will give an example for the multiplicative superposition of a straight periodic cosinusoidal grating and a circular periodic-like cosinusoidal grating. The transmittance functions of these two gratings are given by

$$\begin{cases} r_1(x,y) = \frac{1}{2}\cos\left(\frac{2\pi}{T_1}x\right) + \frac{1}{2} \\ r_2(x,y) = \frac{1}{2}\cos\left(\frac{2\pi}{T_2}\sqrt{x^2+y^2}\right) + \frac{1}{2} \end{cases}, \tag{24}$$

where $T_1 : T_2 = 1/P(P \geq 1)$. These situations are shown in Fig. 1.

According to Amidror's study [11], when T_1 is equal to T_2, the (1, ±1) moiré becomes parabolic. If T_2 is slightly larger than T_1, the (1, ±1) moiré becomes hyperbolic; if, however, T_1 is slightly larger than T_2, the (1, ±1) moiré becomes elliptic. In Fig. 1(a), the superposition presents as absolutely parabolic; the generated moiré is evidently the real moiré [(1, ±1) moiré]. In Fig. 1(e), the superposition presents an obscure parabolic-like (1, ±1) moiré. This moiré is actually the pseudo moiré. In Fig. 1(b), the superposition appears hyperbolic but doesn't show the parabolic or elliptic. This proves that the generated moiré is more adjacent to the real moiré. In Fig. 1(d), the superposition appears elliptic; the pseudo moiré becomes more prominent. In Fig. 1(c),

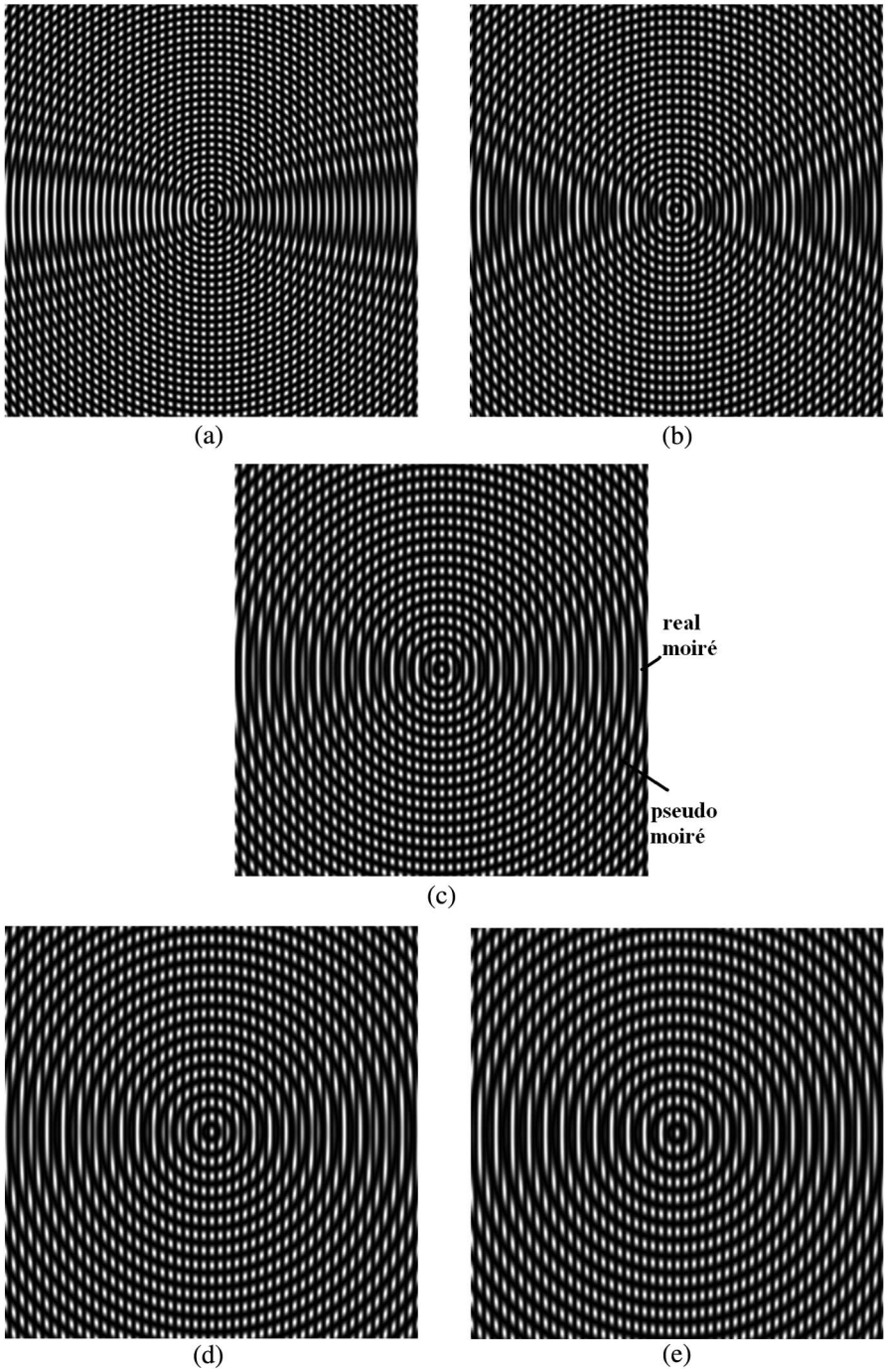

Fig. 1. Multiplicative superposition of straight cosinusoidal grating and circular grating. (a) Period ratio 1:1. (b) Period ratio 1:1.2. (c) Period ratio 1:1.5. (d) Period ratio 1:1.8. (e) Period ratio 1:2.

the superposition presents the obscure coexistence of the elliptic and hyperbolic.

A universal conclusion summarizing this phenomenon would give a supplement for the interpretation in 2.D. When the ratio $T_2:T_1$ (the ratio ≥ 1) approaches 1 (in our example, the ratio can be considered as the threshold), the real moiré is more prominent; when the ratio approaches 2, the pseudo moiré becomes more prominent. When the ratio approaches 1.5, the pseudo and real moirés will be nearly equal to the human eye.

4. Discussion of the Multiplicative Superposition of Binary Repetitive, Periodic-like Gratings

A curvilinear grating with a symmetric square-wave function with period T and opening τ can be expressed in a form of the Fourier series decomposition:

$$r(x,y) = p(g(x,y)) = a_0 + 2\sum_{n=1}^{\infty} a_n \cos\left(\frac{2n\pi g(x,y)}{T}\right), \quad \left(a_0 = \frac{\tau}{T}, a_n = \frac{1}{n\pi}\sin\left(\frac{\pi m\tau}{T}\right)\right). \tag{25}$$

Here, we have

$$\begin{cases} r_1(x,y) = a_0^1 + 2\sum_{m=1}^{\infty} a_m^1 \cos\left(\frac{2n\pi g_1(x,y)}{T_1}\right) \\ r_2(x,y) = a_0^2 + 2\sum_{n=1}^{\infty} a_n^2 \cos\left(\frac{2n\pi g_2(x,y)}{T_2}\right) \end{cases}. \tag{26}$$

The multiplicative superposition of these two binary gratings can be expressed as

$$\begin{aligned} & r_1(x,y) \times r_2(x,y) \\ &= a_0^1 a_0^2 + 2a_0^2 \sum_{m=1}^{\infty} a_m^1 \cos\left[\frac{2\pi m g_1(x,y)}{T_1}\right] \\ &\quad + 2a_0^1 \sum_{n=1}^{\infty} a_n^2 \cos\left[\frac{2\pi n g_2(x,y)}{T_2}\right] \\ &\quad + 2\sum_{m=1}^{\infty}\sum_{n=1}^{\infty} a_m^1 a_n^2 \cos 2\pi\left[\frac{m g_1(x,y)}{T_1} \pm \frac{n g_2(x,y)}{T_2}\right]. \end{aligned} \tag{27}$$

The $(k_1, \pm k_2)$ moiré terms are isolated by the last two new generated terms,

$$\begin{aligned} m_{k_1,\pm k_2} &= 2\sum_{m=-\infty}^{\infty}\sum_{n=-\infty}^{\infty} a_m^1 a_n^2 \\ &\quad \times \cos 2\pi\left[\frac{m g_1(x,y)}{T_1} \pm \frac{n g_2(x,y)}{T_2}\right] \\ &= 2\sum_{n'=1}^{\infty} a_{n'k_1}^1 a_{n'k_2}^2 \cos 2\pi n' \\ &\quad \times \left(\frac{k_1 g_1(x,y)}{T_1} \pm \frac{k_2 g_2(x,y)}{T_2}\right). \end{aligned} \tag{28}$$

The coefficients are expressed as

$$\begin{cases} a_0^1 = \frac{\tau_1}{T_1}, a_m^1 = \frac{1}{m\pi}\sin\left(\frac{\pi m\tau_1}{T_1}\right) = \frac{1}{n'k_1\pi}\sin\left(\frac{\pi n'k_1\tau_1}{T_1}\right) \\ a_0^2 = \frac{\tau_2}{T_2}, a_n^2 = \frac{1}{n\pi}\sin\left(\frac{\pi n\tau_2}{T_2}\right) = \frac{1}{n'k_2\pi}\sin\left(\frac{\pi n'k_2\tau_2}{T_2}\right) \end{cases}. \tag{29}$$

When $k_1 = k_2$, the generated moiré is the $(1, \pm 1)$ moiré. Then we have

$$a_1^1 = \frac{1}{\pi}\sin\left(\frac{\pi\tau_1}{T_1}\right) \quad \text{and} \quad a_1^2 = \frac{1}{\pi}\sin\left(\frac{\pi\tau_2}{T_2}\right). \tag{30}$$

The conditions $0 < \tau_1/T_1 < 1$ and $0 < \tau_2/T_2 < 1$ are always satisfied, so a_1^1 and a_1^2 are always not equal to zero. Therefore, the $(1, \pm 1)$ moiré is always the real moiré, no matter what the opening ratio is.

For $k_1 \neq k_2$, when $n'k_1\tau_1/T_1 = N$ or $n'k_2\tau_2/T_2 = N$ (N is an arbitrary integer), $a_{n'k_1}^2$ or $a_{n'k_2}^2$ will be equal to zero. This makes the $(k_1, \pm k_2)$ moiré the pseudo moiré. On the contrary, the $(k_1, \pm k_2)$ moiré is the real moiré when both $a_{n'k_1}^2$ and $a_{n'k_2}^2$ are not equal to zero.

An example of superposition by a square-wave, periodic-like repetitive grating and a periodic linear grating will be given. The first grating is a binary straight grating with the period T_1, and the second grating is a binary circle grating with the period T_2, where $T_1:T_2 = 1/P(P \geq 1)$. The first superposition is shown in Fig. 2(a), where $T_1:T_2 = 1:1$, $\tau_1/T_1 = 1/2$, and $\tau_2/T_2 = 1/2$. The second superposition is shown in Fig. 2(b), where $T_1:T_2 = 1:2$, $\tau_1/T_1 = 1/2$, and $\tau_2/T_2 = 1/2$.

In Fig. 2(a), the moiré form presents as parabolic. By our discussion, the generated moiré is the real moiré. We can easily mark two curves which are along the orientation of the parabolic path (the generated moiré orientation). It is clear that the average intensities of these two waveforms on the curves vary. A similar analysis would apply in Fig. 2(b); the moiré form is also parabolic but it is the pseudo moiré. According to our previous calculation, the pseudo moiré would present similar characteristics, especially in the orientation. Therefore, the pseudo moiré orientation would easily be obtained by the magnification of the period ratio on the real moiré orientation. We could mark two curves along the pseudo moiré orientation. Furthermore, the average intensities of two waveforms on two parabolic curves are proven to stay constant by our calculation.

Figure 2(a) shows two curves along the moiré orientation to stand for two waveforms of the moiré waveform family. It can be easily seen that the average intensities of waveform 1 and waveform 2 are different. Figure 2(b) also presents two curves along the moiré orientation. However, the average intensities of these waveforms are equal to each other and stay constant. The example confirms that our interpretation and conclusion is also suitable for square or sawtooth waves in repetitive, periodic-like grating superposition.

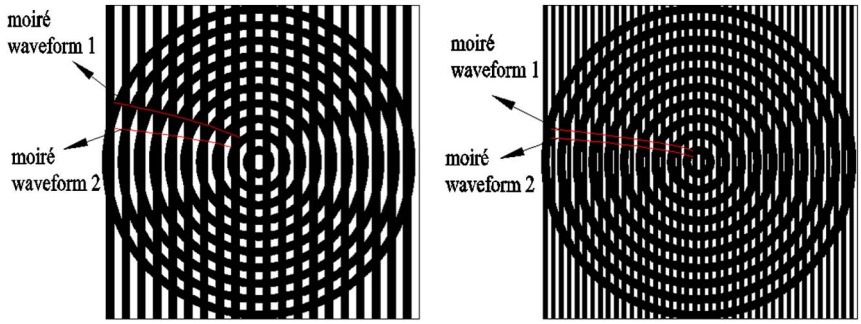

Fig. 2. Multiplicative superposition of straight binary grating and circular grating. (a) Real moiré. (b) Pseudo moiré.

5. Conclusions

This work presents following research and points of view:

(1) The instantaneous parameters period and orientation could be used to describe the generated moiré in multiplicative superposition by two cosinusoidal repetitive, periodic-like gratings in the image domain. They present intuitive mathematical forms of parameters.

(2) The Fourier series expansion presents the basic discrimination of real moiré and pseudo moiré. With the analysis, the parameters of periods and orientations calculated in (1) have been sorted into real and pseudo moiré patterns.

(3) By the combination of these two criteria, the "equivalent period contribution threshold" concept is provided. With the thresholds, the average intensities of generated waveforms along different moiré orientations have been calculated by the mathematical integral method. This shows that different thresholds would make average intensities of waveforms reveal different profiles (cosinusoidal or constant) in different moiré patterns. The interaction of the average intensity distribution and local intensity variation can be considered as macrostructure versus microstructure effects, which introduce confusion to the human eye and produce different visible moiré.

(4) The previous methods give a mathematical interpretation for real and pseudo moiré in the repetitive, periodic-like grating superposition. The theory is novel and reasonable for similar superposition.

(5) An interesting conclusion is that the real moiré and pseudo moiré may coexist in the same superposition. When the threshold distributes in (1, 1.5), the human eye will more easily capture the real moiré. When the threshold distributes in (1.5, 2), the human eye will more easily capture the pseudo moiré orientation. When the threshold is near 1.5, the real moiré and pseudo moiré seem equal to the human eye.

(6) According to the examples in Sections 3 and 4, the interpretation is adapted to various situations such as cosinusoidal, square, sawtooth or other periodic-profile forms in the repetitive, periodic-like grating superposition. Furthermore, it is consistent with the Fourier theory and is understandable in the image domain.

References

1. Lord Rayleigh, "On the manufacture and theory of diffraction-gratings," Philos. Mag. **47**(310), 81–93 (1874). Also published in G. Indebetouw and R. Czarnek, *Selected Papers on Optical Moiré and Applications*, **64**, SPIE Milestone Series (SPIE, 1992), pp. 3–15.
2. S. Kohayashi, *Handbook on Experimental Mechanics*, 2nd ed. (SEM, 1993).
3. K. Patorski, *Handbook of the Moire Fringe Technique* (Elsevier, 1993).
4. H. Takasaki, "Moiré topography," Appl. Opt. **9**, 1467–1472 (1970).
5. I. Amidror and R. D. Hersch, "Fourier-based analysis and synthesis of moirés in the superposition of geometrically transformed periodic structures," J. Opt. Soc. Am. A **15**, 1100–1113 (1998).
6. G. Lebanon, "Variational approach to moiré pattern synthesis," J. Opt. Soc. Am. A **18**, 1371–1382 (2001).
7. I. Amidror and R. D. Hersch, "The role of Fourier theory and of modulation in the prediction of visible moiré effects," J. Mod. Opt. **56**, 1103–1118 (2009).
8. L. Kong, S. Cai, Z. Li, G. Jin, S. Huang, K. Xu, and T. Wang, "Interpretation of moiré phenomenon in the image domain," Opt. Express **19**, 18399–18409 (2011).
9. K. Patorski, K. Pokorski, and M. Trusiak, "Fourier domain interpretation of real and pseudo-moiré phenomena," Opt. Express **19**, 26065–26078 (2011).
10. L. Yu, S.-R. Wang, and G.-Y. Lin, "An image domain approach to the interpretation of the visible moiré phenomenon," J. Opt. **15**, 1–11 (2013).
11. I. Amidror, *The Theory of the Moire Phenomenon* (Springer-Verlag, 2009).
12. M. Abolhassani and M. Mirzaei, "Unification of formulation of moiré fringe spacing in parametric equation and Fourier analysis methods," Appl. Opt. **46**, 7924–7926 (2007).